

Self-Assembling Peptide Solution Accelerates Hemostasis

Tiffany Carter,^{1,2,†} Guangyan Qi,^{1,†} Weiqun Wang,³ Annelise Nguyen,⁴ Nikki Cheng,⁵ Young Min Ju,⁶ Sang Jin Lee,⁶ James J. Yoo,⁶ Anthony Atala,⁶ and Xiuzhi Susan Sun^{1,6,7,*}

- ¹Bio-Materials and Technology Lab, Grain Science and Industry, Kansas State University, Manhattan, Kansas, USA.
- ²Department of Agriculture, Austin Peay State University, Clarksville, Tennessee, USA.
- ³Human Nutrition, Kansas State University, Manhattan, Kansas, USA.
- ⁴Diagnostic Medicine and Pathology, Kansas State University, Manhattan, Kansas, USA.
- ⁵Pathology, University of Kansas Medical Center, Kansas City, Kansas, USA.
- ⁶Wake Forest Institute of Regenerative Medicine, School of Medicine, Wake Forest University, Winston-Salem, North Carolina, USA.
- ⁷Biological and Agricultural Engineering, Kansas State University, Manhattan, Kansas, USA.
- [†]These authors contributed equally to the study.

Objective: One of the leading causes of death following traumatic injury is exsanguination. Biological material-based hemostatic agents such as fibrin, thrombin, and albumin have a high risk for causing infection. Synthetic peptide-based hemostatic agents offer an attractive alternative. The objective of this study is to explore the potential of h9e peptide as an effective hemostatic agent in both *in vitro* and *in vivo* models.

Approach: *In vitro* blood coagulation kinetics in the presence of h9e peptide was determined as a function of gelation time using a dynamic rheometer. *In vivo* hemostatic effects were studied using the Wistar rat model. Results were compared to those of the commercial hemostatic product $Celox^{TM}$, a chitosan-based product. Adhesion of h9e peptide was evaluated using the platelet adhesion test. Biocompatibility of h9e peptide was studied *in vivo* using a mouse model.

Results: After h9e peptide solution was mixed with blood, gelation started immediately, increased rapidly with time, and reached more than 100 Pa within 3s. Blood coagulation strength increased as h9e peptide wt% concentration increased. In the rat model, h9e peptide solution at 5% weight concentration significantly reduced both bleeding time and blood loss, outperforming Celox. Preliminary pathological studies indicate that h9e peptide solution is biocompatible and did not have negative effects when injected subcutaneously in a mouse model.

Innovation: For the first time, h9e peptide was found to have highly efficient hemostatic effects by forming nanoweb-like structures, which act as a preliminary thrombus and a surface to arrest bleeding 82% faster compared to the commercial hemostatic agent Celox.

Conclusion: This study demonstrates that h9e peptide is a promising hemostatic biomaterial, not only because of its greater hemostatic effect than commercial product Celox but also because of its excellent biocompatibility based on the *in vivo* mouse model study.

Keywords: peptide, hydrogel, hemostasis, animal model, wound healing, coagulation



Xiuzhi Susan Sun, PhD

Submitted for publication June 4, 2020. Accepted in revised form June 8, 2020.

*Correspondence: Biomaterials and Technology Laboratory, Grain Science and Industry, Kansas State University, 101 BIVAP Building, 1980 Kimball Avenue, Manhattan, KS 66506, USA (e-mail: xss@ksu.edu).

INTRODUCTION

Exsanguination is one of the leading causes of death in traumatic injuries. ^{1–7} The human body addresses bleeding by the process of hemostasis (the coagulation cascade), ⁸ which is not always adequate to control the amount of bleeding during traumatic injuries. To assist with the body's natural process of hemostasis, research has been conducted over the past 40 years on hemostatic agents, several of which have become commercially available.

Hemostatic agents stop bleeding either through their own mechanical methods or by reinforcing the coagulation cascade. Most of the hemostatic agents currently available on the market are derived from biological sources, including, but not limited to, purified bovine serum albumin, bovine thrombin, fibrin, and crustacean chitin. Because the components of these homeostatic agents are obtained from biological sources, allergic reaction or infection from contaminated biological systems is a common concern. S,12

Self-assembling peptides offer an attractive alternative because these peptides possess the ability to form nanofibers and/or hydrogels and have shown promise in wound healing and hemostasis. 13-15 Compared with biological hemostatic agents, synthetic peptides reduce the risk of negative immune response and infection. Charbonneau et al. used the ideal amphipathic peptide (IAP), a peptide sequence composed of only lysine and leucine residues (KLLKLL), coupled with a biocompatible polymer hydrogel matrix surface to form a hemostatic material. 15 Their study indicated that the use of IAP reduced bleeding time from 250 s (negative control) to 180s in a rabbit ear model and was potentially safer than the commercial zeolite powder agent QuikClot. 15 Ruan et al. created nanowebs using an amphiphilic peptide sequence (N-PSFCFKFEP-C) that contains proline (P) residues at both terminals, which add turning function of the sequence, and therefore can link peptide components to arrest bleeding faster than both 1% chitosan solution and gauze. 14 Others peptides, such as the collagen-mimicking peptide (Pro-Lys-Gly)4(Pro-Hyp-Gly)4(Asp-Hyp-Gly)₄, also showed improved hemostatic control. ¹⁶

Among the existing peptide-based hemostatic materials, the most popular is RADA₁₆ (AcN-RADARADARADARADA-CONH₂). The RADA₁₆ peptide sequence is composed of alternating hydrophobic and hydrophilic amino acid residues that, in an aqueous environment, possess the ability to form a stable β -sheet structure. Recently, Cheng *et al.* added tyrosine-isoleucine-glycine-serine-arginine and glycine-arginine-glycine-

aspartic acid-serine motifs to RADA₁₆, to improve its functionality.¹³ They found that both the motifadded version and the original RADA₁₆ sequence possessed the ability to induce hemostasis, with no significant difference in effect.¹³ However, the acidic isoelectronic pH of RADA₁₆-based peptides may cause local inflammation.^{13,17,18} A safer peptide than RADA was designed and named T45K. When it comes into contact with blood, T45K utilizes the charges from amino acids to form a barrier to block blood flow and achieve hemorrhage control within a few seconds to a few minutes.¹⁹ However, T45K does not adhere to or interact with blood components, so bleeding could easily reoccur. The formed barrier also requires pressure, stitches, or gauze wrapping.

Recently, Sun and Huang developed a highly biocompatible and safe peptide named h9e, which combines two native protein domains: the β -spiral motif of the spider flagelliform silk protein²⁰ and the calcium binding motif of the human muscle protein.²¹ Under neutral pH at room or body temperature, h9e can self-assemble into nanofibers and then transform into a sol-gel reversible hydrogel through shearing force such as pipetting or syringing.^{21,22} H9e and its derived hydrogels have been used primarily for three-dimensional cultures of various cancer cells^{23–26} and secondarily for safe *in vivo* delivery of drugs, antigens, and viruses.^{27–29}

One of our earlier studies also showed that h9e formed hydrogel when mixed with blood serum, suggesting a hemostatic effect. The objective of this study is to explore the potential of h9e as a hemostatic agent in both *in vitro* and *in vivo* models. As study results showed, when h9e peptide solution was mixed with blood, gelation started immediately. Compared with the commercial hemostatic agent CeloxTM (a chitosan-based product), h9e solution at a peptide concentration higher than 5% formed hydrogel faster in a rat model and reduced both bleeding time and blood loss. H9e peptide solution is biocompatible and did not have negative effects when injected subcutaneously in a mouse model.

CLINICAL PROBLEM ADDRESSED

Hemorrhage is one of the leading causes of death in traumatic injury. For decades, hemostatic agents have been developed to stop bleeding. Hemostatic agents currently available on the market include, but are not limited to, purified bovine serum albumin, bovine thrombin, fibrin, chitosan, and gelatin-based products. These products have low hemostatic efficiency and can cause inflam-

mation and allergy. Although synthetic fibrin or collagen proteins have recently been investigated and evaluated, to date, their hemostatic function has not been confirmed. Self-assembling peptides offer an attractive alternative because peptides possess the ability to form nanofibers and/or hydrogels and have shown promise in wound healing and hemostasis. To date, no peptide-based hemostatic agent is available due to either strong adhesion or no adhesion or acidic pH. In this study, we propose a novel h9e peptide that forms nanoweb-like structures at a physiological pH and temperature, is biocompatible, and causes no potential damage to surrounding tissues.

MATERIALS AND METHODS

Materials and animals

As described in Carter, 30 h9e peptide was synthesized at the Biomaterials and Technology Laboratory at Kansas State University following the procedure by Huang et al. 22 The purity of the h9e peptide used was ≥85% as confirmed by highperformance liquid chromatography. H9e peptide solutions at 1%, 3%, and 5% peptide concentrations by weight were prepared by dissolving the freezedried peptide powder in 100 mM NaHCO₃. Wistar rat whole blood and Wistar rat blood components were purchased from Innovative Research (Novi, MI). Male Wistar rats for *in vivo* bleeding studies and Friend leukemia virus B (FVB) female mice for pathological studies were ordered from Charles River Laboratories International (Wilmington, MA). Moore Medical CELOXTM Hemostatic Granules was

obtained from Medtrade Products Ltd. (Electra House, Crewe, UK).

Coagulation kinetics

As described by Carter,³⁰ time sweep dynamic rheology was conducted on the mixture of h9e solutions (at 1, 3, and 5 wt% peptide concentrations) and Wistar rat whole blood or blood components (serum, plasma, and red blood cells) at a mixing ratio of 1:1 to yield final h9e concentrations of 0.5%, 1.5%, and 2.5%. Two hundred microliters of the appropriate wt% of the h9e peptide solution was added to $200 \,\mu\text{L}$ of Wistar rat whole blood or its components in a small vial. The mixture was homogenized and immediately added to the rheometer for evaluation. The elastic modulus G' of the h9e/blood hydrogel was determined using a C-VOR 150 rheometer (Malvern Instruments, Malvern, Worcestershire, UK). A plate 20 mm in diameter was used with 1% strain and 1Hz frequency at 37°C temperature for 30 min.

In vivo hemostatic efficiency in rat model

As described by Carter, ³⁰ similar to the method used by Mortazavi *et al.*, 30 rats were randomly divided into 5 groups of 6 animals each.⁵ Male Wistar rats were kept on an AIN-93 diet with free access to water and under 12 h-light/12-h dark cycles for one week. Before their tails were excised, the rats were anesthetized and maintained with 3% isoflurane (Fig. 1, arrow A) until the eyelid closure reflex was lost and there was no reactive reflex in response to a toe pinch. To maintain the rats' appropriate body temperatures during anesthesia, a circulating water blanket was used at a

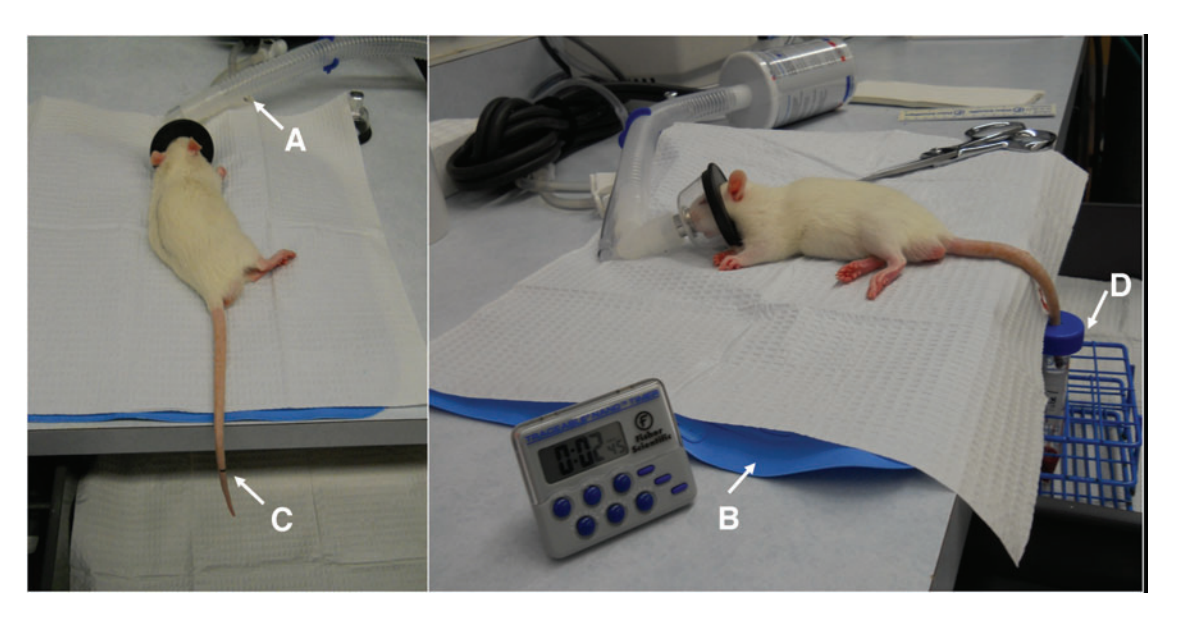


Figure 1. Illustration of hemorrhage *in vivo* experiment to determine bleeding time and amount (A 3% isoflurane; B water blanket with temperature of 41–43°C; C Rat tail; D vial containing different treatment). Color images are available online.

temperature of 41–43°C (Fig. 1, arrow B). Following anesthesia, animals' tails were cut off at a thickness of 5 mm using a pair of mortuary scissors (Fig. 1, arrow C). The cut tail was immediately inserted into a small vial containing different treatment (Fig. 1, arrow D). The 1st group received topical saline solution (negative control) and the 2nd to 4th groups received topical h9e peptide solutions at 1, 3, and 5 wt% concentrations, respectively. The 5th group received topical application of a commercially available hemostatic agent as a positive control (Moore Medical CELOX Hemostatic Granules, Medtrade Products Ltd., Electra House). After treatment, the volume of blood loss was measured using a scaled test tube. Bleeding time was measured using a stopwatch. Before the procedure was performed, the weight of each animal and the mean weight of animals used in each testing group were recorded. At the conclusion of the study, the rats were sacrificed using a carbon dioxide chamber. All animal testing was done in accordance with procedures approved by the Institutional Animal Care and Use Committee (IACUC protocol no. 3276) at Kansas State University.

Morphological imaging

At high concentration, h9e is viscous with thick nanofibers. Therefore, for all imaging experiments, 0.5% wt concentration of h9e was used to clearly observe its interactions with blood components.

Transmission electron microscopy. As described by Carter, 30 the morphology of rat blood and 1% h9e solution (1:1 ratio) with final h9e concentration of 0.5% was observed using transmission electron microscopy (TEM). Exactly 6 mL of the samples was placed onto a negative glow discharge carbon-coated copper grid for 2 min. The remaining sample was removed by blotting with a Kimwipe (Kimberly Clark Professional, Roswell, GA). The grid was then placed into 2% uranyl acetate for 2 min. Extra stain was removed by blotting with tissue paper. The wet grids were allowed to air dry for several minutes before being examined under TEM. Samples were imaged using an FEI Technai G2transmission electron microscope at an electron acceleration voltage of 200 KeV. Images were captured using a standardized, normative electron dose and a constant defocus value from the carboncoated surfaces.

Confocal microscopy. As described by Carter, 30 10 μ L of rat blood and 1% h9e solution (1:1 ratio) with final h9e concentration of 0.5% were placed onto a glass slide and covered with a cover slip. The

samples were observed under an Olympus spinning disk confocal inverted microscope, and images were captured using slide book version 5.5 (3i-Intelligent Imaging Innovations, Inc., Tokyo, Japan).

Atomic force microscopy. As described by Carter, 30 morphology of rat blood and h9e solution was observed using Innova Atomic Force Microscope (AFM; Bruker, Camarillo, CA) in the Biomaterials and Technology Laboratory, Department of Grain Science and Industry, Kansas State University. Ten microliters of rat blood and 1% h9e solution (1:1 ratio) with final h9e concentration of 0.5% were placed evenly on the surface of a clean mica slide. The sample was allowed to dry on the slide for roughly 60 s. The slide was then rinsed using $100\,\mu\mathrm{L}$ of distilled water. Rinsing was repeated 3 times. The sample was then placed in a covered Petri dish to air dry. The microstructure images were scanned using the contact mode with a Burker's sharp nitride lever probe. The probe combines the sharpness of a silicon tip with a low spring constant of 0.12 N/m and a nominal tip radius of ~ 2 nm. Experiments were carried out in air at a scan rate of 2 Hz, and a vertical deflection of 2 V was applied. All AFM images with 512×512 pixels were obtained.

Platelet adhesion test

Fresh human platelet-rich plasma (PRP) containing an anticoagulant was supplied by Zen-Bio, Inc. (Research Triangle Park, NC). The platelet concentration of PRP was 10×10^6 platelets/mL as counted by a hemocytometer. H9e solution with concentration of 0%, 1%, 3%, and 5% was mixed with a gel trigger solution (PGworks, PepGel LLC) at a ratio of 5.25:1. The mixtures were precoated onto a 4-well chamber slide system and set at 37°C for 30 min. PRP was prewarmed to 37°C and added to the 4-well chamber slide. After 120-min incubation at 37°C, the wells were washed three times with phosphate-buffered saline (PBS) (fresh PBS each time) with mild shaking to remove nonadherent platelets. For scanning electron microscopy (SEM) examination (Model 2250N; Hitachi, Japan), platelets adhering to the h9e-coated surfaces were fixed with 2.5% glutaraldehyde (Gibco Laboratories, USA) for 20 min at room temperature. After thorough washing with PBS, the platelets were freezedried overnight. Platelet-attached surfaces were gold deposited in vacuum and examined by SEM. Platelet density on the surfaces was also estimated by SEM. Different fields were randomly counted and values were expressed as the average number of adhered platelets per high-power field.

Biocompatibility test with in vivo mouse model

Subcutaneous injection and tissue fixation. ment was injected subcutaneously into the mammary fat pad of FVB mice. Three groups of three animals each were used. One group received 1% of h9e solution in PBS (200 μ L per animal), one group received PBS only (200 μL per animal), and one group received no-injection treatment. Implantation of the h9e peptide solution was monitored for 2 weeks, and tissues were harvested on day 14. Mammary fat pads at the inguinal region were removed and fixed in a solution of 4% formaldehyde and embedded into paraffin before being sectioned into $5 \mu m$ thickness for immunohistochemistry analysis. Husbandry of animals is conducted by the Comparative Medical Group (CMG) at the College of Veterinary Medicine at Kansas State University. Animal care and use protocols were approved by the IACUC at Kansas State University (Protocol Number: 3643).

Immunohistochemistry. Five micron sections were dewaxed and subjected to antigen retrieval under low-pressure heating for 2 min in 1 M urea for chemokine (C-C motif) ligand 2 (CCL2), 2 M urea pH6.8 for transforming growth factor beta (TGF- β), or 10 mM sodium citrate pH 6.0 for all other antigens. Endogenous peroxidases were quenched by incubation in a PBS buffer containing 20% methanol/3% H_2O_2 . For TGF- β , slides were processed for 3,3'-diaminobenzidine staining using the Mouse on Mouse Kit (cat. no. BMK-2202; Vector Laboratories) according to the manufacturer's instructions. For other antigens, slides were blocked in PBS/3% fetal bovine serum and then incubated overnight in a blocking buffer with primary antibodies at 1:100 dilution to arginase-1 (cat. no. 20150; Santa Cruz Biotechnology), αsmooth muscle actin (α-sma, cat. no. 7187; Abcam), F4/80 (cat. no. ab6640; Abcam), and Von Willebrand Factor 8 (VWF8; cat. no. Ab7356; Millipore), or 1:5 dilution to fibroblast-specific protein 1 (FSP1; cat. no. 75550; Abcam). To detect arginase-1, α-sma, FSP1, and VWF8, slides were incubated with secondary rabbit biotinylated antibodies at a 1:1,000 dilution for 2 h. To detect CCL2, slides were incubated with secondary anti-goat biotinylated antibodies at a 1:1,000 dilution. Secondary antibodies were bound to streptavidin-peroxidase (cat. no. PK-4000; Vector Laboratories) and incubated with 3,3'-diaminobenzidine substrate (cat. no. SK-4100; Vector Laboratories). Slides were counterstained in Mayer's hematoxylin for 1 min, dehydrated, and mounted with Cytoseal. Five images

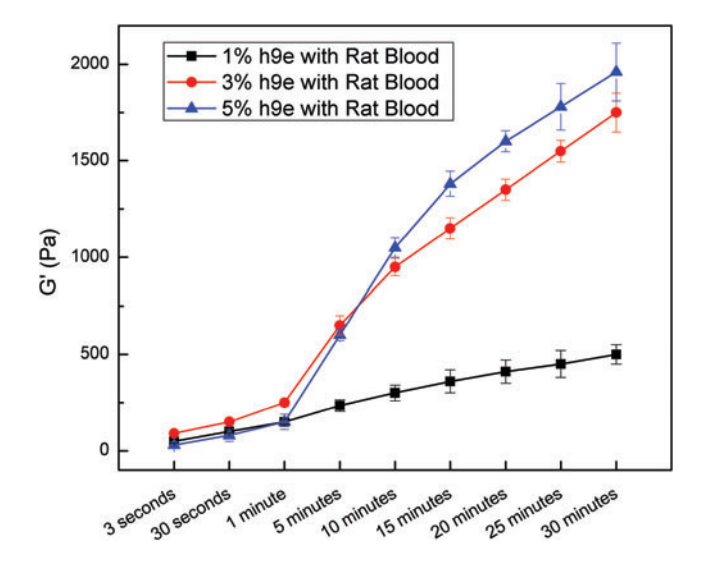


Figure 2. Time sweep test: storage modulus versus time of Wistar rat whole blood samples with 1%, 3%, and 5% h9e peptide concentrations (1:1 ratio of blood to h9e solution). Color images are available online.

per slide per sample were captured at 10×magnification using an FL Auto Imaging System (Invitrogen). Immunostaining was quantified by ImageJ using methods previously described.³¹

Statistical analysis

Data from experiments carried out in triplicate were analyzed through analysis of variance and least significant difference at the 0.05 level according to procedures in the SAS statistical software package (SAS Institute 2005, Cary, NC).

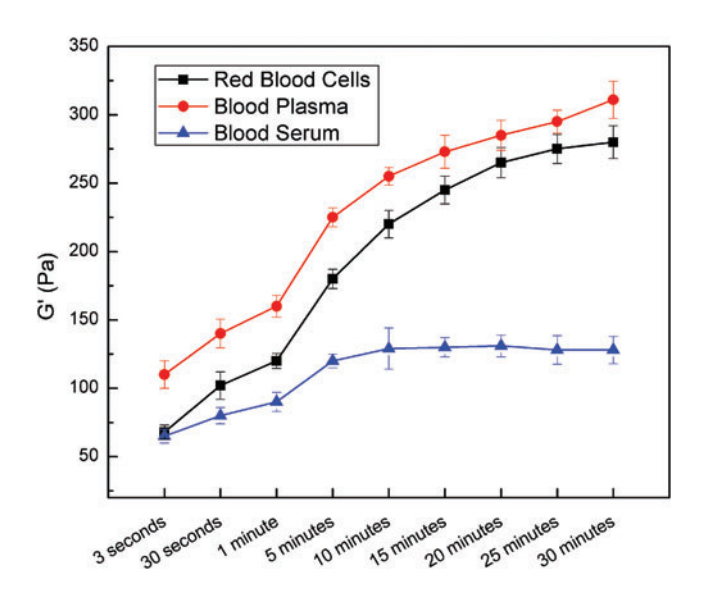


Figure 3. Storage modulus versus time of Wistar rat blood components with 1% h9e peptide (1:1 ratio of blood components to h9e solution). Color images are available online.

Table 1. Average weight of rats, blood loss evaluation, and time evaluation for hemostatic effect

Test Group	Animal Body Weight (g)	Blood Loss (mL)	Bleeding Time (seconds)
Saline (negative control)	245.85*	2.76*	521.33*
1% h9e solution	239.33*	2.20*	203.33**
3% h9e solution	252.05*	1.87*	226.00**
5% h9e solution	253.45*	0.75**	94.00***
Celox™ (positive control)	254.91*	1.53*	225.20**

Means with different asterisks in the same column are significantly different at $p \le 0.05$.

RESULTS

Coagulation kinetics

H9e peptide solutions at all concentrations (1%, 3%, and 5%) formed hydrogel immediately after mixing with Wistar rat whole blood samples at 1:1 mixing ratio (final h9e concentration was 0.5%, 1.5%, and 2.5%, respectively) (Fig. 2). Gel strength reached above 100 Pa within 3 s for all h9e peptide concentrations. Gel strength of h9e at 3% and 5% peptide concentrations had a sharp increase at 1 min, reached about 1,700 and 1,900 Pa respectively by 30 min, and continued increasing afterward. The high elastic modulus (G') indicates strong interactions between h9e peptide and blood and strong coagulation, which suggest that h9e peptide at 3% concentration and above has a significant hemostatic effect.

To examine which blood components interacted with h9e solution and led to coagulation, we investigated the coagulation kinetics of h9e at 1% peptide concentration with Wistar rat blood serum, plasma, and red blood cells at a ratio of 1:1 (final h9e con-

centration was 0.5%). Figure 3 shows that a gelation response was induced with all three components. Gel strength reached up to 310, 280, and 125 Pa within 30 min for red blood cells, blood plasma, and blood serum, respectively. Since blood serum is obtained by intentionally removing the body's natural clotting factors from blood plasma, the difference in gel strength between plasma and blood serum samples was attributed to the clotting factors. Given the coagulation strength (~ 500 Pa) of h9e at 0.5% final peptide concentration at 30 min with Wistar rat whole blood (Fig. 2), red blood cells, and blood plasma (including clotting factors and blood serum), all contributed to h9e's coagulation effect. So

In vivo hemostatic effect in rat model

H9e solutions at all peptide concentrations (1%, 3%, and 5%) showed hemostatic effects compared to the sterile saline negative control (Table 1). As the concentration of h9e solution increased, hemostatic effect significantly increased as judged by blood loss (Table 1). Five percent h9e solution was able to control bleeding most effectively with the lowest blood loss (0.75 mL), significantly outperforming ($p \le 0.05$) the commercial positive control hemostatic agent Celox granules (1.53 mL blood loss). Furthermore, 5% h9e solution was the most efficient hemorrhage control agent, achieving a 94-s average bleeding time, again significantly outperforming ($p \le 0.05$) Celox granules (about 225 s).

Morphological observations

Under AFM, h9e solution and Wistar whole blood mixture showed a uniform structure with randomly distributed small particles (Fig. 4A).

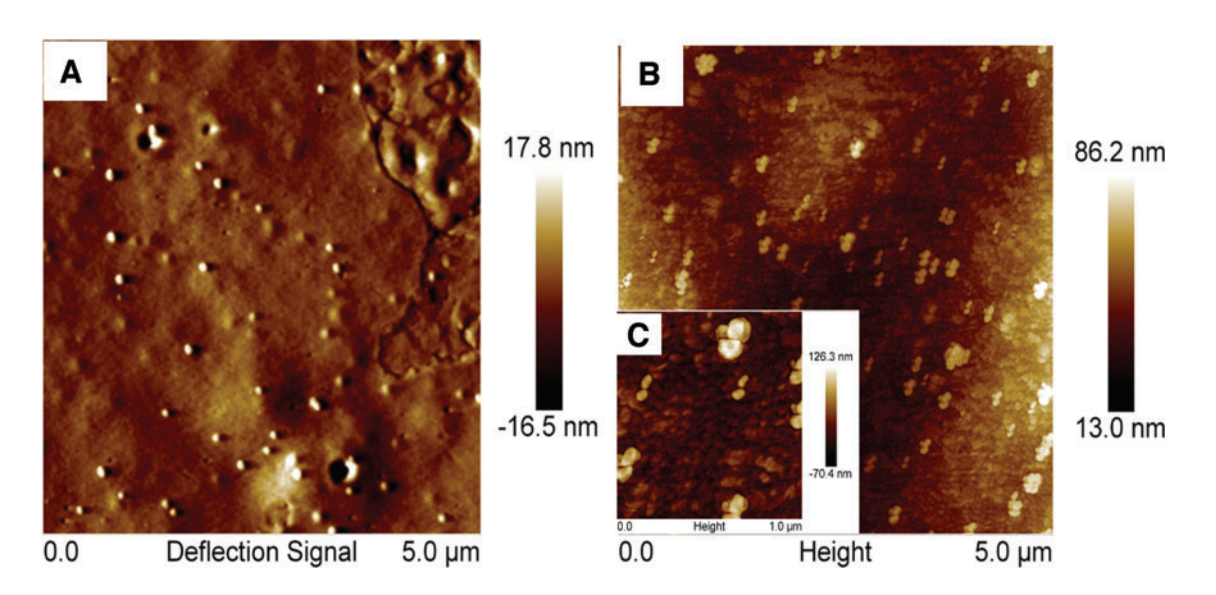


Figure 4. AFM images of rat blood sample and 1% h9e solution (1:1 ratio) with final h9e concentration of 0.5%. (A) Contact image shows particles. (B) Tapping image shows that particles are small clusters. (C) Closer view of the small particle clusters. AFM, atomic force microscopy. Color images are available online.

Under close observation, the small particles are aggregate clusters (Fig. 4B, C). TEM images showed that h9e peptide hydrogels formed fibrous networks (Fig. 5A, B), which is in agreement with published data. ^{22,23,29} Given this fibrous network, the uniform structure shown in the AFM images must have a very dense surface. This suggests strong interactions between h9e and blood that created an entangled fibrous network resulting in a

solid surface. Judging by the successful hemorrhage control in the rat *in vivo* study, we assumed that the hydrogel formed from h9e solution and blood provided an effective sealing surface; moreover, the small aggregate clusters may have allowed clotting factors to attach to the surface.

As described by Carter,³⁰ h9e solution formed aggregates with blood proteins and other components in the serum and plasma (Fig. 5C–F). There

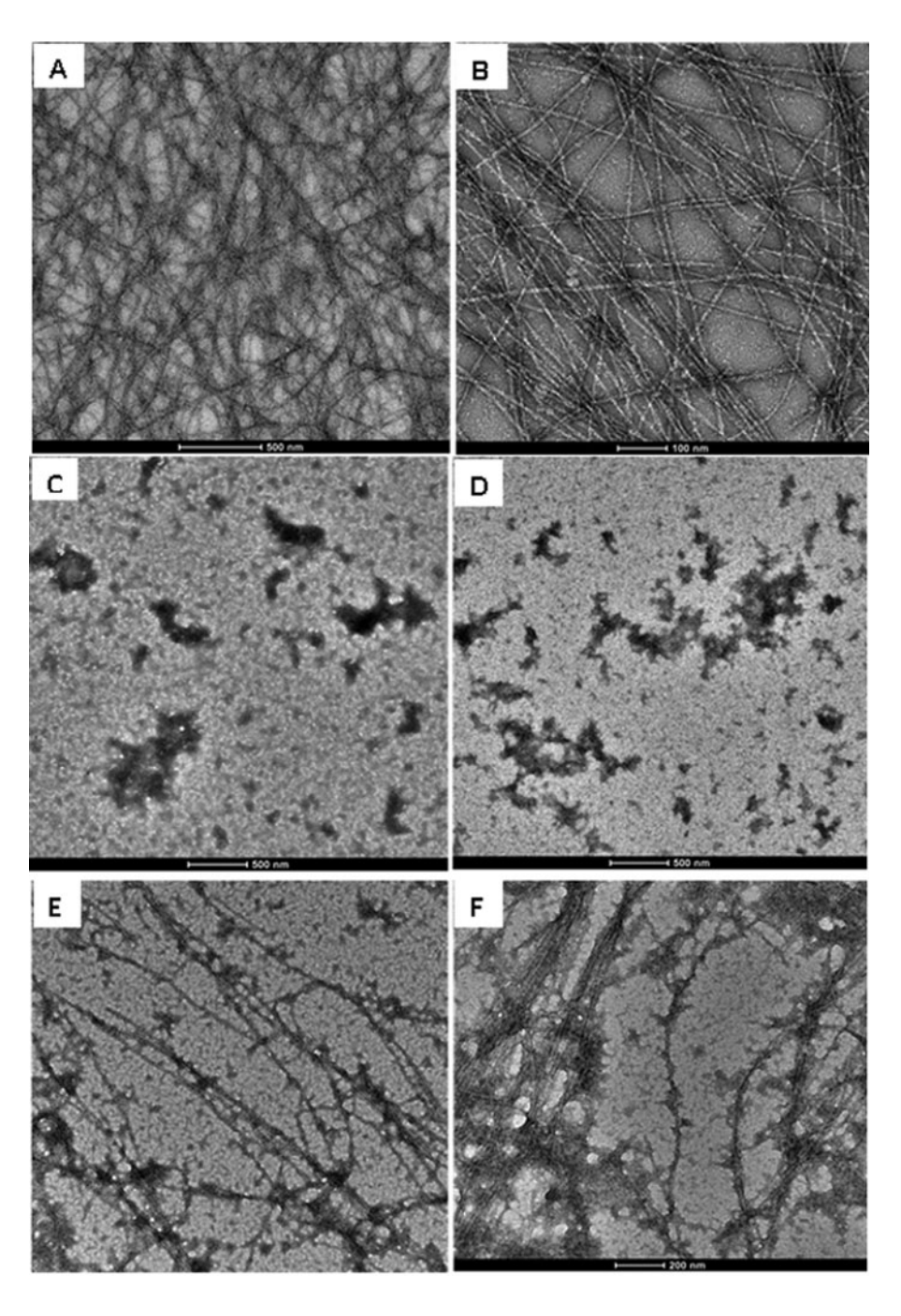


Figure 5. TEM images of (A) 0.5% h9e peptide solution at 500 nm scale; (B) 0.5% h9e peptide solution at 100 nm scale; (C) Wistar rat blood serum alone; (D) Wistar rat blood plasma alone; (E) Wistar rat blood serum with 0.5% h9e (1:1 ratio of serum to 1% h9e); and (F) Wistar rat blood plasma with 0.5% h9e (1:1 ratio of plasma to 1% h9e). TEM, transmission electron microscopy.

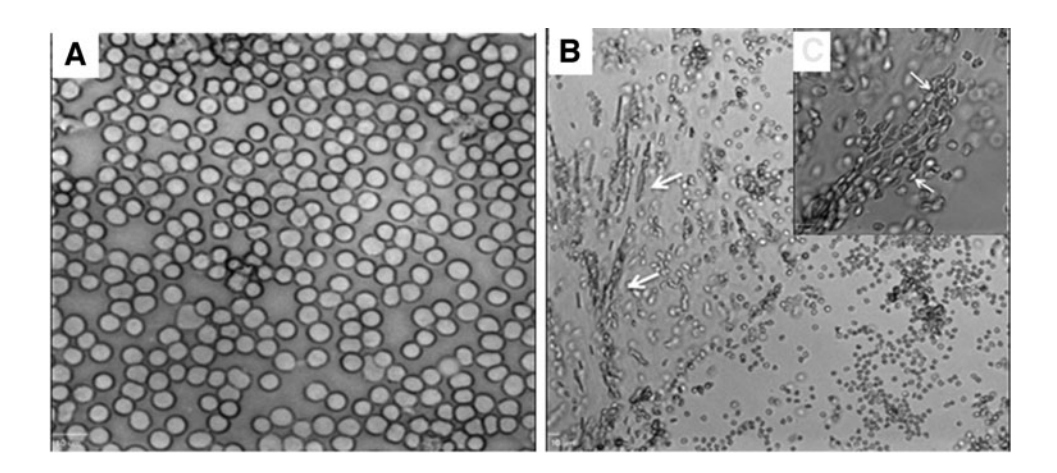


Figure 6. Confocal images of (A) untreated red blood cells; (B) red blood cells with 0.5% h9e solution (1:1 ratio of cells to 1% h9e); and (C) red blood cells with 0.5% h9e solution (1:1 ratio of cells to 1% h9e) at higher magnification. The arrows indicate immobilized cells within the nanoweb.

is clear binding of blood serum components to h9e fibers (Fig. 5E). Similar binding of plasma components to h9e fibers was observed (Fig. 5F). By contrast, Fig. 6A shows red blood cells suspended freely in saline. When red blood cells were added to 0.5% h9e peptide solution, as shown in Fig. 6B, the cells became trapped within the h9e fiber nanoweb. The arrows in Fig. 6C indicate immobilized cells within the nanoweb. These morphological results confirmed the coagulation rheological findings that blood plasma, serum, and red blood cells are all important factors attributing to h9e's hemostatic effect.

Biocompatibility test in vivo mouse model

Foreign substances and chronic diseases such as cancer can induce an inflammatory reaction in the mammary gland, characterized by increased cytokine expression, angiogenesis, recruitment of immune cells, and fibrosis. 32–34 To determine the effect of h9e solution on the mammary gland, fixed tissues were immunostained for expression of CCL2 and TGF- β inflammatory cytokines^{35–38}; VWF8, an angiogenesis marker^{39,40}; arginase-1, an M2 macrophage marker⁴¹; and α -smooth muscle actin and FSP1, two fibroblast markers. 42,-45 FSP1 expression was significantly lower in PBS- and h9e solution-treated mammary glands than in untreated glands, but there were no significant differences in the expression of inflammatory biomarkers between PBS- and h9e solution-treated mammary glands (Fig. 7; Table 2). Saline solutions are generally considered nontoxic and commonly used to resuspend biological materials for in vivo delivery. 46,47 Some studies also indicate that saline solutions can modulate fibroblast activity and immune response, 48,49 including exerting antiinflammatory effects.⁵⁰ While no studies have been reported on the effects of PBS on the adult mammary gland, the doses and duration of treatment in this study could have contributed to the differences in FSP1 expression among groups. Regardless, these results indicate that the administration of h9e solution does not exert any more effects on the microenvironment than PBS and does not induce inflammation in the mammary gland. In addition, mice weight and external body temperature were measured daily and showed no deviation within 2 weeks of h9e solution injection. No lesion was observed at injection sites.

DISCUSSION

This study provides the first observation of h9e peptide being highly efficient as a potential hemostatic agent. H9e is an amphiphilic peptide and self-assembles into nanofibers that can form a nanoweb-like structure (Fig. 8). Amphiphilicity as a physiochemical property has been known to induce hemostatic responses by activating some of blood's natural clotting factors. Nanoweb-like structures are known to seal bleeding surfaces in a typical wound, preventing hemorrhage and rapidly inducing hemostasis. ⁵¹

H9e fibers are reinforced by blood components within the blood plasma, as shown in TEM images (Fig. 5).³⁰ Red blood cells are entangled with h9e fibers, as shown in confocal images (Fig. 6).³⁰ In addition, metal ions such as calcium and sodium, although very low in blood, can promote h9e peptide gelation.²⁷ Collectively, these cause a strong gelation response and the formation of a structure similar to that of a blood clot (Fig. 8). The structure can act as both a preliminary thrombus and a

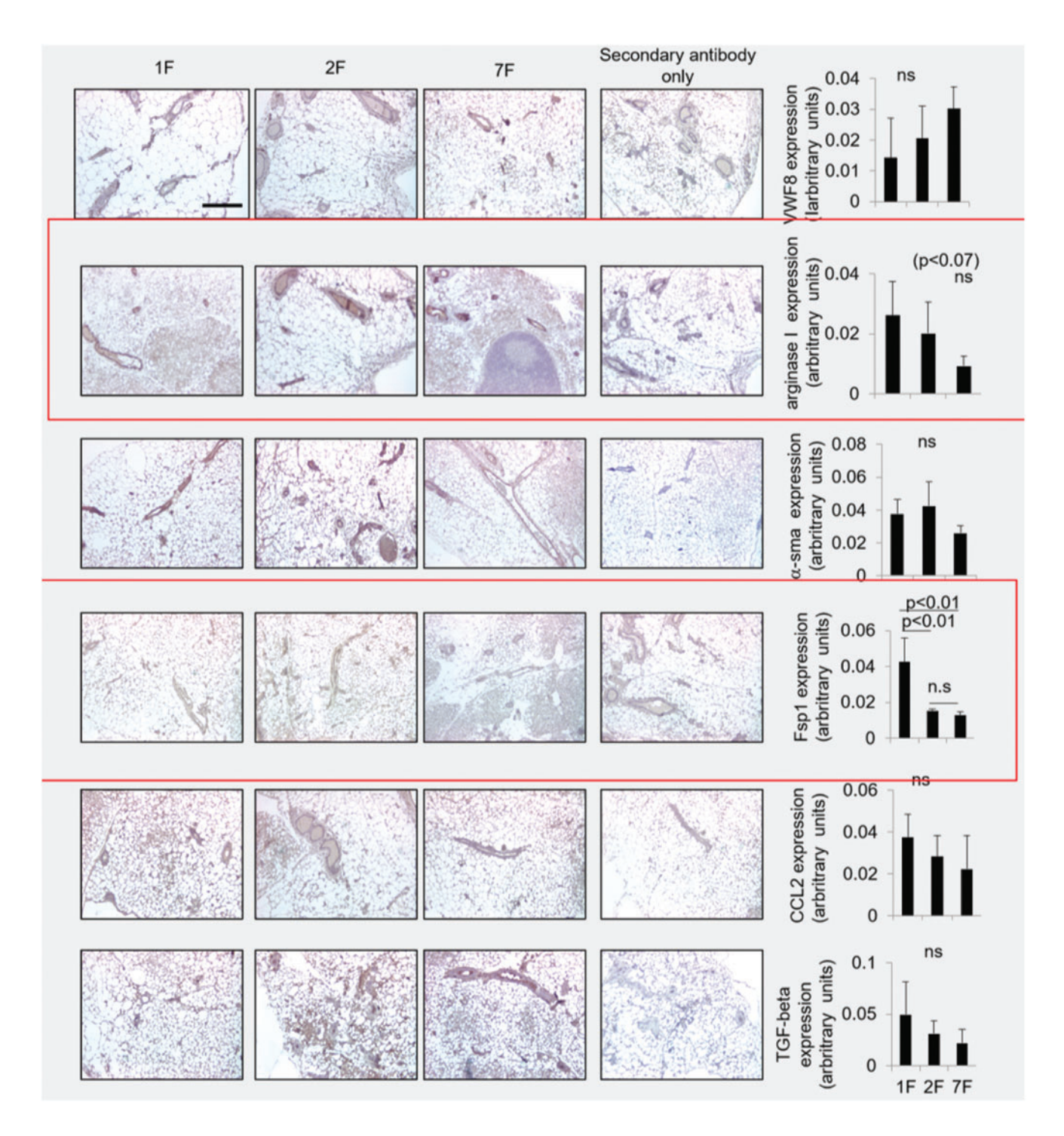


Figure 7. H9e peptide does not affect the expression of inflammatory markers in the mammary gland. Native (untreated, 1F), PBS-treated (2F), and 1% h9e solution (7F)-treated mammary glands were immunostained for expression of the indicated proteins. Expression was quantified by ImageJ and normalized to hematoxylin staining. Statistical analysis was performed using one-way ANOVA with Bonferroni post hoc comparison. Statistical significance was determined by p < 0.05. Scale bar= 400 μ m. ANOVA, analysis of variance; ns, not significant; PBS, phosphate-buffered saline. Color images are available online.

surface upon which a thrombus can continue to develop until bleeding is arrested.³⁰ The nanoweb structure formed by h9e peptide entangled with blood is similar to a fibrin within the coagulation cascade, mimicking the nanoweb-like structure of fibrin and its ability to maintain a blood clot.

Furthermore, h9e peptide does not have strong adhesion to blood components, so blood components are not damaged during the formation of nanoweblike structures. In our platelet adhesion test, the numbers of platelets adhering to the surface of h9e-coated chamber slides were lower than those

Table 2. Inflammation analysis (ImageJ arbitrary unit) of fixed tissue isolated from the mice injection site: 1F= without treatment, 2F= treated with PBS buffer, and 7F= treated with 1% h9e solution

	1F	2F	7F	796 FVB normal mammary gland
VWF8	0.015	0.020	0.030	0.050
Arginase-1	0.027	0.02	0.008	0.034
α-sma	0.038	0.042	0.026	0.020
FSP1	0.042	0.015	0.014	0.036
CCL2	0.038	0.028	0.025	0.024
TGF- β	0.050	0.030	0.022	0.020

Seven hundred ninety-six FVB normal mammary gland was used as standard reference.

CCL2, chemokine (C–C motif) ligand 2; FSP1, fibroblast-specific protein 1; FVB, Friend leukemia virus B; α -sma, α -smooth muscle actin; TGF- β , transforming growth factor beta; VWF8, Von Willebrand Factor 8.

adhering to noncoated chamber slides (control) at all peptide concentrations tested (Fig. 9). In another experiment, according to morphological images, red blood cells maintained their "biconcave disc" shape without shrinking or eryptosis for up to at least 10 days in 0.5% h9e peptide hydrogel. On the other hand, based on *in vitro* protease (i.e., trypsin) tests, different protease enzyme degraded h9e hydrogel in a matter of hours or days; h9e degradation rate was affected by protease doses. In addition, in a subcutaneously injection for *in vivo* biocompatibility study, we observed a small bump at the injection site that disappeared in about a week, leaving no lesion or inflammation, which suggests that h9e peptide hydrogel can be de-

graded by proteases found in biological systems in about a week (Result not shown). The immuno-histochemistry studies described in this study (Fig. 7; Table 2) showed no negative pathological effect. Based on these findings, we speculate that the h9e and blood-entangled nanoweb structure can be easily removed, absorbed, or degraded at the interface between the nanoweb and the injury tissue surface, and can advance healing with minimal scarring.

As described by Carter, 30 commercially available Celox granules boast the ability to induce hemostasis in the presence of an anticoagulant. This was confirmed by an experimental study performed by Koksal et al. 52 In the study, Celox induced hemostasis in the presence of an orally administered warfarin anticoagulant. The study also indicated that Celox has the ability to clot blood under hypothermic conditions.⁵² Although rats used in our study were not treated with an oral anticoagulant, the blood samples used for the rheology study (Fig. 2) were drawn using Alsevers, a balanced isotonic salt solution and an anticoagulant. Thus, we speculate that h9e is also able to induce hemostasis in the presence of an anticoagulant. Further studies are needed to confirm this hypothesis.

Compared with most other published peptides with potential for hemostasis, ^{17,19} h9e is biocompatible, pH neutral, bioabsorbable, fibrin nanoweb structure mimicking, and noncytotoxic *in vivo*, and has no side effects according to the mouse model

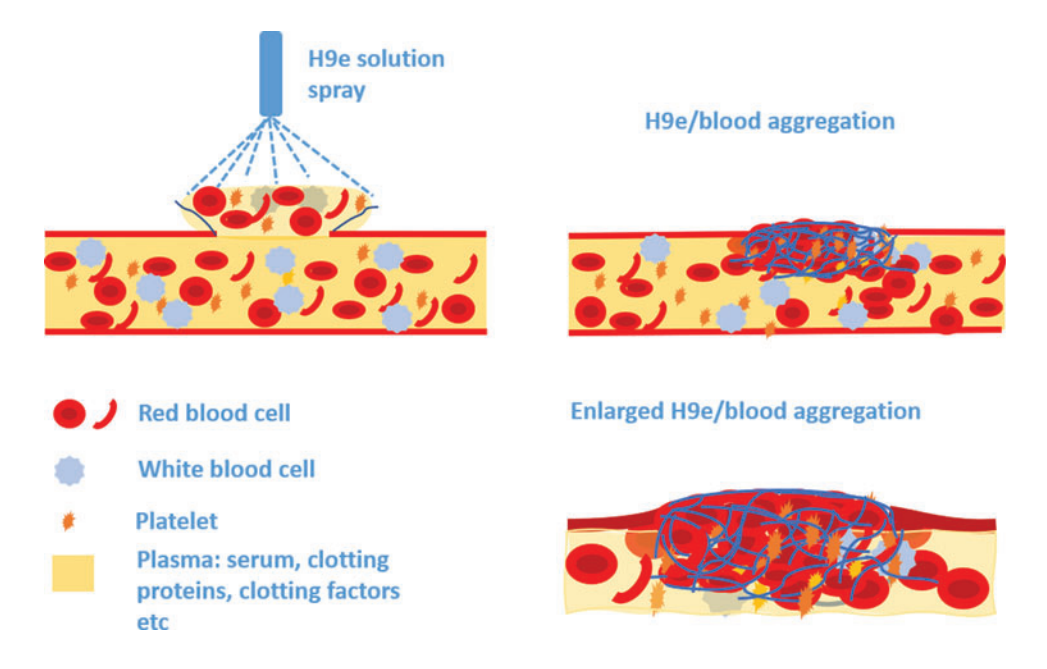


Figure 8. Diagram of h9e peptide blood clotting mechanism. CCL2, chemokine (C–C motif) ligand 2; TGF- β , transforming growth factor beta. Color images are available online.

studies. The h9e peptide sequence contains no biological element, which eliminates the risk of infection from contaminated biological sources. ^{52,53} Furthermore, h9e gel can be degraded and/or absorbed in about a week *in vivo*. In *in vitro* rheology studies, h9e peptide solutions coagulated with blood samples and at 3 and 5 wt% formed gels strong enough to arrest bleeding. This hemostatic effect was confirmed in an

in vivo rat model where h9e at 5 wt% peptide concentration saved 73% blood in 94 s and was 82% faster to arrest bleeding than the commercial hemostatic agent Celox, which saved 45% blood in 225 s at 57% rate of hemorrhage.

All in all, H9e peptide can form nanoweb-like structures when mixed with all blood components, including plasma, serum, and red blood cells. This nanoweb-like structure, mimicking the fibrin nanoweb, may act as both a preliminary thrombus and a surface upon which a thrombus can continue to develop until bleeding is arrested. This study indicates that h9e peptide is a promising hemostatic biomaterial.

INNOVATION

Current hemostatic agents are mostly from biological sources, $^{9-11}$ which can cause allergic reaction or infection. 8,12 RADA $_{16}$ peptide is one of the most attractive peptide-based hemostatic agents to reduce contamination; however, the acidic isoelec-

KEY FINDINGS

- H9e peptide delivers greater and faster hemostatic effect compared to commercial hemostatic agent Celox.
- Red blood cell and blood plasma (i.e., clotting factors, serum) all contribute to h9e's hemostatic effect.
- H9e peptide is biocompatible; it can be degraded in about a week in mouse and does not induce inflammation in the mammary gland.

tronic pH of RADA $_{16}$ causes local inflammation. 13,17,18 We have recently discovered h9e peptide, which is biocompatible and can self-assemble into nanofibers and form a sol-gel reversible hydrogel under physiological pH and temperature. 21,22 This study, for the first time, demonstrated that h9e peptide, at a certain concentration, coagulated rapidly with blood components and formed a nanoweblike structure to arrest bleeding.

ACKNOWLEDGMENTS AND FUNDING SOURCES

Part of this study was originally undertaken as a master's thesis. Thus, portions of the Materials and Methods, Results, and Discussion section from this document are incorporated into this article. The authors would like to thank the Comparative Medical Group at Kansas State University College of Veterinary Medicine for their support and assistance. Authors also appreciate the financial support from USDA/KS Agricultural Experimental Station.

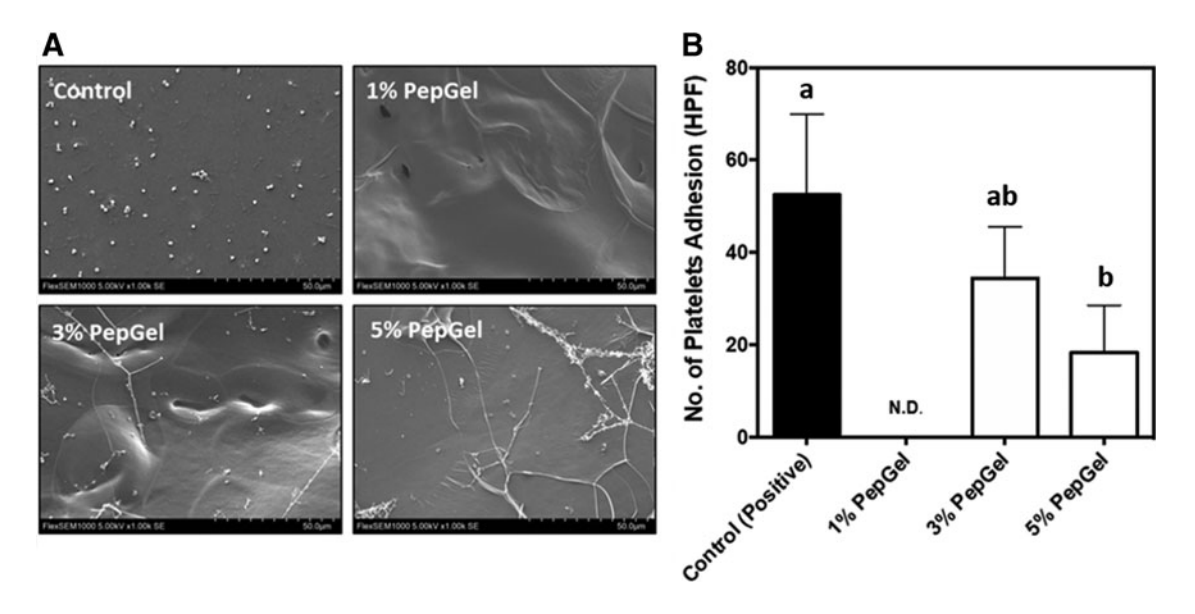


Figure 9. Platelet adhesion to h9e at 0%, 1%, 3%, and 5% peptide concentrations: (A) SEM images; (B) quantitative analysis of SEM imaging data. Values are mean \pm SD of triplicate experiments. Means with different superscripts are significantly different at $p \le 0.05$. HPF, high power field; SD, standard deviation; SEM, scanning electron microscopy.

AUTHOR DISCLOSURE AND GHOSTWRITING

The authors state no competing financial interests. The content of this article was expressly written by the authors listed. No ghostwriters were used to write this article.

ABOUT THE AUTHORS

Tiffany Carter, PhD, was a master's student in the Grain Science and Industry Department at Kansas State University and is an assistant professor in the Department of Agriculture at Austin Peay State University. Guangyan Qi, PhD, is postdoc researcher in Grain Science and Industry Department at Kansas State University. Weiqun Wang, PhD, is professor in Human Nutrition Department at Kansas State University. Annelise Nguyen, PhD, is associate professor in the Department of Diagnostic Medicine/Pathobiology at Kansas State University. Nikki Cheng, PhD, is associate Professor in the Department of Pathology and Laboratory Medicine, University of Kansas

Medical Center. Young Min Ju, PhD, is instructor at Wake Forest Institute of Regenerative Medicine, School of Medicine, Wake Forest University. Sang **Jin Lee, PhD,** is associate professor at Wake Forest Institute of Regenerative Medicine, School of Medicine, Wake Forest University. James J. Yoo, PhD, is professor at Wake Forest Institute of Regenerative Medicine, School of Medicine, Wake Forest University. Anthony Atala, PhD, is professor at Wake Forest Institute of Regenerative Medicine, School of Medicine, Wake Forest University. Xiuzhi Susan Sun, PhD, is distinguished professor in Grain Science and Industry Department and Biological and Agricultural Engineering at Kansas State University, and adjunct professor at Wake Forest Institute of Regenerative Medicine, School of Medicine, Wake Forest University.

FUNDING INFORMATION

Funding for this research was provided by Kansas State University.

REFERENCES

- Evans JA, van Wessem KJ, McDougall D, Lee KA, Lyons T, Balogh ZJ. Epidemiology of traumatic deaths: comprehensive population-based assessment. World J Surg 2010;34:158–163.
- Kozen BG, Kircher SJ, Henao J, Godinez FS, Johnson AS. An alternative hemostatic dressing: comparison of CELOX, HemCon, and QuikClot. Acad Emerg Med 2008;15:74–81.
- Kheirabadi B, Klemcke HG. Hemostatic agents for control of intracavitary non-compressible hemorrhage: An overview of current results. In: RTO HFM Symposium, St. Pete Beach, FL, 2004.
- Bellamy RF. The causes of death in conventional land warfare: implications for combat casualty care research. Mil Med 1984;149:55–62.
- Mortazavi SM, Atefi A, Roshan-Shomal P, Raadpey N, Mortazavi G. Development of a novel mineral based haemostatic agent consisting of a combination of bentonite and zeolite minerals. J Ayub Med Coll Abbottabad 2009;21:3–7.
- Champion HR, Bellamy RF, Roberts CP, Leppaniemi A. A profile of combat injury. J Trauma Inj Infect Crit Care 2003;54:S13–S19.
- Hoyt DB, Bulger EM, Knudson MM, et al. Death in the operating room: an analysis of a multi-center experience. J Trauma Acute Care Surg 1994;37: 426–432.

- Traver MA, Assimos DG. New generation tissue sealants and hemostatic agents: innovative urologic applications. Rev Urol 2006;8:104–111.
- Cheng CM, Meyer-Massetti C, Kayser SR. A review of three stand-alone topical thrombins for surgical hemostasis. Clin Ther 2009;31:32–41.
- Shabanova EM, Drozdov AS, Fakhardo AF, Dudanov IP, Kovalchuk MS, Vinogradov VV. Thrombin@Fe304 nanoparticles for use as a hemostatic agent in internal bleeding. Sci Rep 2018;8:233.
- Baker JE, Goodman MD, Makley AT, et al. Evaluation of a novel fibrin sealant patch in hemorrhage control after vascular or hepatic injury. Mil Med 2018;184:e290–e296.
- Raccuia JS, Simonian G, Dardik M, Hallac D, Raccuia SV, Stahl R, Dardik H. Comparative efficacy of topical hemostatic agents in a rat kidney model. Am J Surg 1992;163:234–238.
- Cheng TY, Wu HC, Huang MY, Chang WH, Lee CH, Wang TW. Self-assembling functionalized nanopeptides for immediate hemostasis and accelerative liver tissue regeneration. Nanoscale 2013;5:2734.
- 14. Ruan L, Zhang H, Luo H, Liu J, Tang F, Shi YK, Zhao X. Designed amphiphilic peptide forms stable nanoweb, slowly releases encapsulated hydrophobic drug, and accelerates animal

- hemostasis. Proc Natl Acad Sci U S A 2009;106: 5105–5110.
- Charbonneau S, Lemarié CA, Peng HT, Ganopolsky JG, Shek PN, Blostein MD. Surface-attached amphipathic peptides reduce hemorrhage in vivo. J Trauma Acute Care Surg 2011;72:136–142.
- Kumar VA, Taylor NL, Jalan AA, Hwang LK, Wang BK, Hartgerink JD. A nanostructured synthetic collagen mimic for hemostasis. Biomacromolecules 2014;15:1484–1490.
- Zhang S, Gelain F, Zhao X. Designer selfassembling peptide nanofiber scaffolds for 3D tissue cell cultures. Semin Cancer Biol 2005;15: 413–420.
- Xu FF, Wang YC, Sun S, Ho AS, Lee D, Kiang KM, et al. Comparison between self-assembling peptide nanofiber scaffold (SAPNS) and fibrin sealant in neurosurgical hemostasis. Clin Transl Sci 2015; 8:490–494.
- Rahmani G, Prats J, Norchi T, Kates S, McInerney V, Woods J, Kelly J. First safety and performance evaluation of T45K, a self-assembling peptide barrier hemostatic device, after skin lesion excision. Dermatol Surg 2018;44:939–948.
- Huang H, Sun XS. Rational design of responsive self-assembling peptides from native protein sequences. Biomacromolecules 2010;11:3390–3394.

- 21. Sun XS. Huang, H. Novel protein peptide hydrogels. USA Patent #8,835,395 2014.
- Huang H, Herrera Al, Luo Z, Prakash O, Sun XS. Structural transformation and physical properties of a hydrogel-forming peptide studied by NMR, transmission electron microscopy, and dynamic rheometer. Biophys J 2012;103:979–988.
- Huang H, Ding Y, Sun XS, Nguyen TA. Peptide hydrogelation and cell encapsulation for 3D culture of MCF-7 breast cancer cells. PLoS One 2013; 8:e59482.
- 24. Kumar D, Kandl C, Hamilton CDA, et al. Mitigation of tumor-associated fibroblast-facilitated head and neck cancer progression with anti-hepatocyte growth factor antibody ficlatuzumab. JAMA Otolaryngol Neck Surg 2015;141:1133.
- Liang J, Sun XS, Yang Z, Cao S. Anticancer drug camptothecin test in 3D hydrogel networks with HeLa cells. Sci Rep 2016;7:1–9.
- Miller PG, Shuler ML. Design and demonstration of a pumpless 14 compartment microphysiological system. Biotechnol Bioeng 2016;113:2213–2227.
- Huang H, Shi J, Laskin J, Liu Z, McVey DS, Sun XS. Design of a shear-thinning recoverable peptide hydrogel from native sequences and application for influenza H1N1 vaccine adjuvant. Soft Matter 2011;7:8905.
- Li X, Galliher-Beckley A, Huang H, Sun X, Shi J. Peptide nanofiber hydrogel adjuvanted live virus vaccine enhances cross-protective immunity to porcine reproductive and respiratory syndrome virus. Vaccine 2013;31:4508–4515.
- Liang J, Liu G, Wang J, Sun XS. Controlled release of BSA-linked cisplatin through a PepGel self-assembling peptide nanofiber hydrogel scaffold. Amino Acids 2017;49:2015–2021.
- Carter T. Hemostatic efficiency of amphiphilic peptide solutionin Wistar Rat model. Thesis, Kansas State University, 2014.
- Fang WB, Yao M, Brummer G, Acevedo D, Alhakamy N, Berkland C, Cheng N. Targeted gene silencing of CCL2 inhibits triple negative breast cancer progression by blocking cancer stem cell renewal and M2 macrophage recruitment. Oncotarget 2016;7:49349–49367.
- Glynn DJ, Hutchinson MR, Ingman WV. Toll-like receptor 4 regulates lipopolysaccharide-induced inflammation and lactation insufficiency in a mouse model of Mastitis1. Biol Reprod 2014;90:91.
- Radisky ES, Radisky DC. Stromal induction of breast cancer: inflammation and invasion. Rev Endocr Metab Disord 2007;8:279–287.

- Walker II, WH, Borniger JC, Zalenski AA, et al. Mammary tumors induce central pro-inflammatory cytokine expression, but not behavioral deficits in Balb/C mice. Sci Rep 2017;7:1–13.
- Palomino DCT, Marti LC, Palomino DCT, Marti LC. Chemokines and immunity. Einstein (São Paulo) 2015;13:469–473.
- Tylaska LA, Boring L, Weng W, Aiello R, Charo IF, Rollins BJ, Gladue RP. Ccr2 regulates the level of MCP-1/CCL2 in vitro and at inflammatory sites and controls T cell activation in response to alloantigen. Cytokine 2002;18:184–190.
- Maskarinec G, Ju D, Fong J, Horio D, Chan O, Loo LW, Hernandez BY. Mammographic density and breast tissue expression of inflammatory markers, growth factors, and vimentin. BMC Cancer 2018;18:1191.
- Santibañez JF, Quintanilla M, Bernabeu C. TGF-β/ TGF-β receptor system and its role in physiological and pathological conditions. Clin Sci 2011;121: 233–251.
- Weidner N. Current pathologic methods for measuring intratumoral microvessel density within breast carcinoma and other solid tumors. Breast Cancer Res Treat 1995;36:169–180.
- Zanetta L, Marcus SG, Vasile J, et al. Expression of von Willebrand factor, an endothelial cell marker, is up-regulated by angiogenesis factors: a potential method for objective assessment of tumor angiogenesis. Int J Cancer 2000;85:281–288.
- Yang Z, Ming X-F. Functions of arginase isoforms in macrophage inflammatory responses: impact on cardiovascular diseases and metabolic disorders. Front Immunol 2014;5:533.
- Strutz F, Okada H, Lo CW, Danoff T, Carone RL, Tomaszewski JE, Neilson EG. Identification and characterization of a fibroblast marker: FSP1. J Cell Biol 1995;130:393–405.
- Lawson WE, Polosukhin VV, Zoia O, et al. Characterization of fibroblast-specific protein 1 in pulmonary fibrosis. Am J Respir. Crit Care Med 2005;171:899–907.
- Yamaoka K, Nouchi T, Marumo F, Sato C. α-Smooth-muscle actin expression in normal and fibrotic human livers. Dig Dis Sci 1993;38:1473–1479.
- Nouchi T, Tanaka Y, Tsukada T, Sato C, Marumo F. Appearance of α-smooth-muscle-actin-positive cells in hepatic fibrosis. Liver 2008;11:100–105.
- Bacci E, Cianchetti S, Paggiaro PL, et al. Comparison between hypertonic and isotonic saline-induced sputum in the evaluation of airway inflammation in subjects with moderate asthma.
 Clin Exp Allergy 1996;26:1395–1400.

- Buffa EA, Lubbe AM, Verstraete FJ, Swaim SF. The effects of wound lavage solutions on canine fibroblasts: an in vitro study. Vet Surg 1997;26:460–466.
- Huynh NCN, Everts V, Leethanakul C, Pavasant P. Ampornaramveth RS. Rinsing with saline promotes human gingival fibroblast wound healing in vitro. PLoS One 2016;11:e0159843.
- 49. Wieczorowska-Tobis K, Polubinska A, Breborowicz A, Oreopoulos DG. A comparison of the biocompatibility of phosphate-buffered saline and dianeal 3.86% in the rat model of peritoneal dialysis. Adv Perit Dial 2001;17:42–46.
- Lichtenauer M, Nickl S, Hoetzenecker K, et al. Phosphate buffered saline containing calcium and magnesium elicits increased secretion of interleukin-1 receptor antagonist. Lab Med 2009;40:290–293.
- Chan LW, Wang X, Wei H, Pozzo LD, White NJ, Pun SH. A synthetic fibrin cross-linking polymer for modulating clot properties and inducing hemostasis. Sci Transl Med 2015;7:277ra29– 277ra29.
- 52. Koksal O, Ozdemir F, Cam Etoz B, Buyukcoskun NI, Sigirli D. Hemostatic effect of a chitosan linear polymer (Celox®) in a severe femoral artery bleeding rat model under hypothermia or warfarin therapy. Ulus Travma Acil Cerrahi Derg 2011;17: 199–204.
- Komatsu S, Nagai Y, Naruse K, Kimata Y. The neutral self-assembling peptide hydrogel SPG-178 as a topical hemostatic agent. PLoS One 2014;9: e102778.

Abbreviations and Acronyms

 $\alpha\text{-sma} = \alpha\text{-smooth muscle actin}$

AFM = atomic force microscopy

ANOVA = analysis of variance

CCL2 = chemokine (C-C motif) ligand 2

CMG = Comparative Medical Group

FSP1 = fibroblast-specific protein 1

FVB = Friend leukemia virus B

HPF = high power field

IACUC = Institutional Animal Care and Use Committee

IAP = ideal amphipathic peptide

ns = not significant

 ${\sf PBS} = {\sf phosphate}\text{-}{\sf buffered} \ {\sf saline}$

PRP = platelet-rich plasma

 $RADA_{16} = AcN-RADARADARADARADA-CONH_2$

SD = standard deviation

SEM = scanning electron microscopy

 $\mathsf{TEM} = \mathsf{transmission} \ \mathsf{electron} \ \mathsf{microscopy}$

 $\mathsf{TGF}\text{-}\beta = \mathsf{transforming}$ growth factor beta

VWF8 = Von Willebrand Factor 8